Applications of synchrotron X-ray imaging in bone research

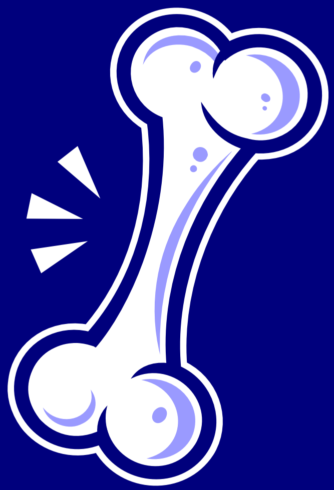

Murielle Salomé

Outline

1. Bone
2. Relevant X-ray Imaging techniques
3. Bone micro-structure
   - 3D bone micro-architecture in (µCT)
   - 3D mineral bone density (quantitative µCT)
   - In vivo µCT
4. Bone mineralisation
   - Apatite maturation (µXANES)
   - Mineral crystallites, collagen fibers (µSAXS)
5. Biomechanics
   - Bone under compressive stress (µCT)
6. Metals accumulation in bone
   - Localisation of La in bone (µXRF)
7. Orthopedics and biomaterials
   - DEI imaging of bone implants
   - Scaffold osseo-integration (µCT, µXRD)
8. FTIR micro-spectroscopy
9. Perspectives

1. Bone

Bone

- Functions
  - Support and protection of the soft tissues and organs
  - Body movement
  - Mineral storage (Ca, P…) and homeostasis
  - Hematopoiesis
- Cortical bone
  - Hard outer layer of bone
  - Closely packed osteons
- Cancellous bone
  - Less dense than cortical bone
  - Honeycomb-like 3D structure
  - Network of plate and bar shaped trabeculae

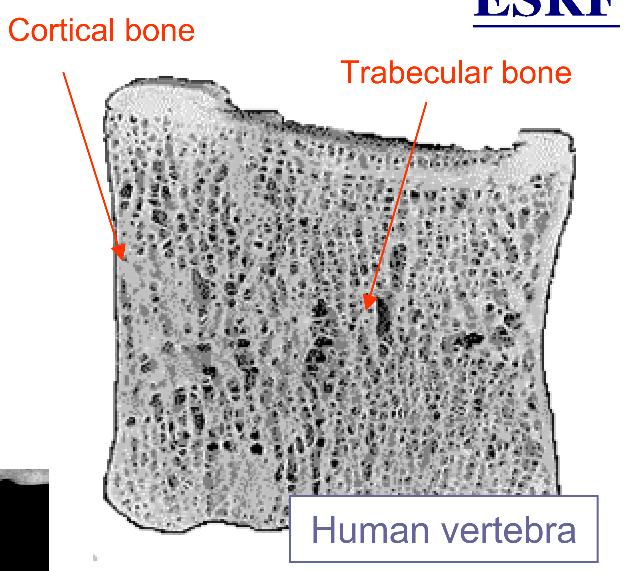

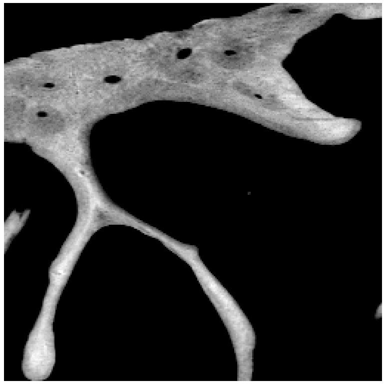

X-ray µCT image of human cortical bone

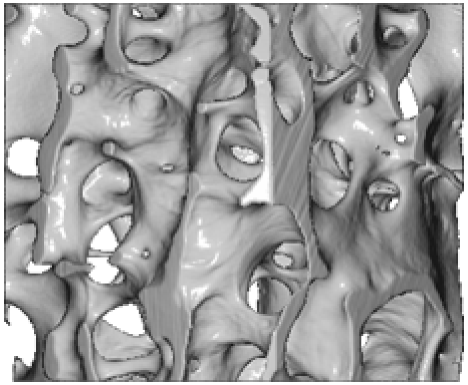

X-ray µCT image of human trabecular bone

M. Salomé *et al*., *Medical Physics* 26(10), 2194-2204, 1999.

Bone tissue – A composite nano-material

- Composite nano-material
  - Collagen fibrils reinforced with mineral platelets
  - Mechanical competences (stiffness and toughness)

- Organic matrix
  - Mainly type I collagen forming a triple helical structure arranged in fibrils (Ø100 nm)
  - Template for mineral phase
  - Some non-collagenous proteins

- Mineral phase
  - Poorly crystalline carbonated apatite
  - Many ion substitutions
  - 2-5 nm thick apatite crystallites
  - Crystals aligned along fibril axis

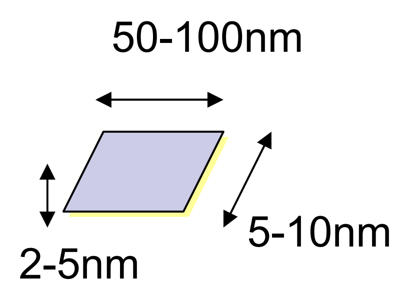

- Bone formation and remodeling
  - Bone continuously resorbed and replaced by new bone
  - Inhomogeneous bone mineralisation: bone regions with different mineral content depending on tissue age

2. Relevant X-ray Imaging techniques

SR X-ray imaging and bone research

Bone micro-structure

- Alteration with age, pathology (osteoporosis, osteoarthritis …), …
- Effects of therapy

High resolution imaging in 2D and 3D (µm / nm)

Metals accumulation in bone

Pb, Al, Sr, La …

Detection of trace elements with high sensitivity (ppm)

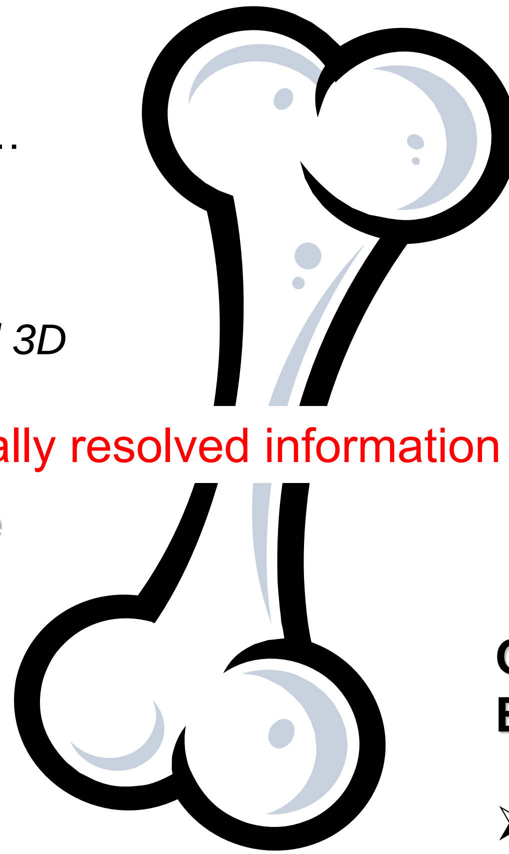

Spatially resolved information

Bone mineralisation

- Identification of mineral phases
- Apatite maturation
- Crystallinity
- Alteration with age, pathology (rickets, osteogenesis imperfecta, osteopetrosis …), …

Chemical speciation
Molecular information
Crystallographic properties

Orthopedics and Biomaterials

- Micro-structure
- Bone integration

Bone mechanical properties

- Bone micro- / nano-structure behavior under strain

SR X-ray imaging and bone research

	Bone micro-structure	Bone mineralisation	Biomechanics	Metals in bone	Orthopedics Biomaterials
X-ray µtomography	Bone micro-architecture in 3D	Mineral density	Structure deformation		Micro-structure Bone integration
X-ray µfluorescence		Ca/P ratio		Localization of trace metals	Diffusion of metals from prosthesis
X-ray µspectroscopy		Apatite maturation		Chemical state	
Infra-red µspectroscopy		Bone mineral phases			Bone integration Material characterization
µSAXS / µXRD		Apatite crystallites	Deformation at the nano-scale		Bone integration
Diffraction Enhanced Imaging	Cartilage structure				Bone integration

In blue: examples developed hereafter

3. Bone micro-structure

Quantification of the 3D micro-architecture of trabecular bone using x-ray microtomography

- 3D Non-destructive imaging technique
- High spatial resolution, tunable from 10 µm to <1 µm
- Access to 3D histomorphometric parameters
  - Bone volume fraction (BV/TV)
  - Bone trabecular thickness (Tb.Th)
  - Trabecular spacing (Tb.Sp)
  - Connectivity parameters
  - Anisotropy
  - …
- Quantitative reconstruction of linear attenuation coefficient in monochromatic beam
  - 3D Bone mineral density
- Dedicated sample environments for *In situ* studies
  - Bone structure deformation and cracks propagation under compressive stress
- *In vivo* studies

Evolution of bone trabecular structure with age

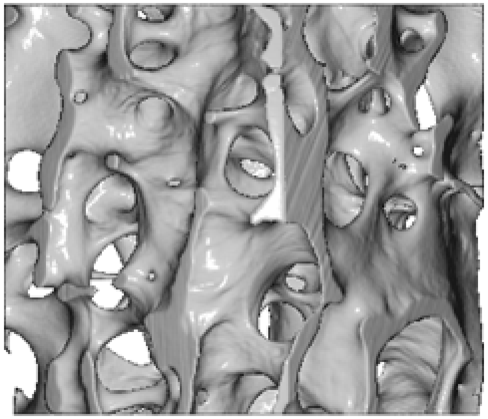

33 year old

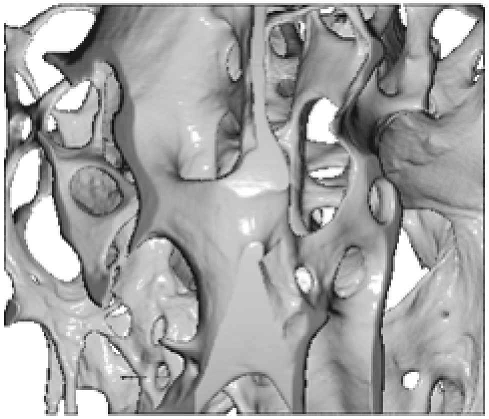

55 year old

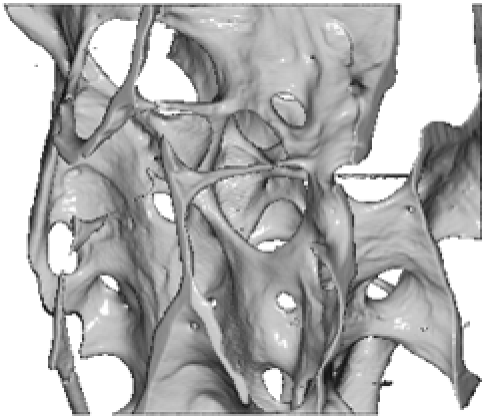

82 year old

1mm

10 vertebral spongiosa samples from women with different ages.

- Decrease of trabecular bone volume with age
- Increase of mean trabecular spacing
- Decrease in connectivity
- No significant thinning of the trabeculae

M. Salomé *et al.*, *Medical Physics* 26(10), 2194-2204, 1999.
F. Peyrin *et al., Cellular and Molecular Biology* 46(6), 1089-1102, 2000.

M. Salomé, ESRF ID21
F. Peyrin, CREATIS INSA Lyon & ESRF ID19

Quantitative measurement of the degree of mineralization in bone

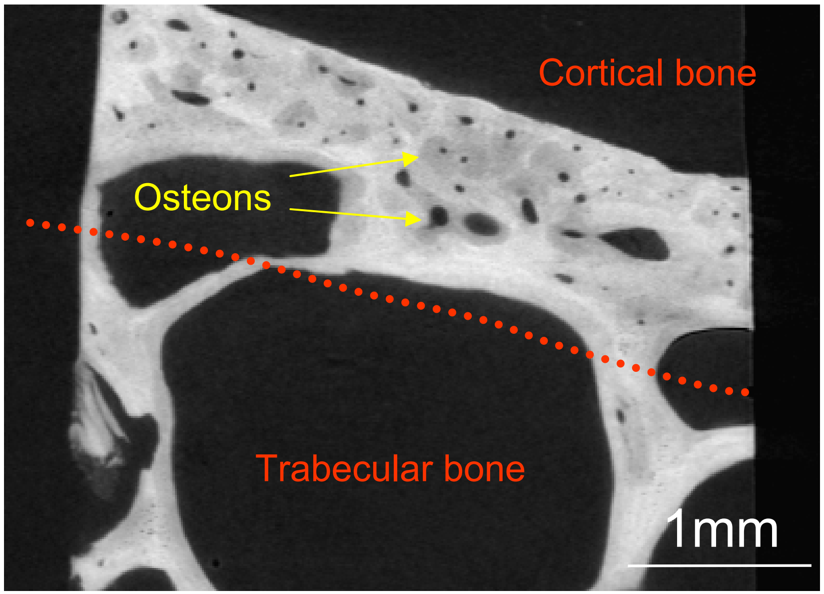

Human iliac crest biopsies

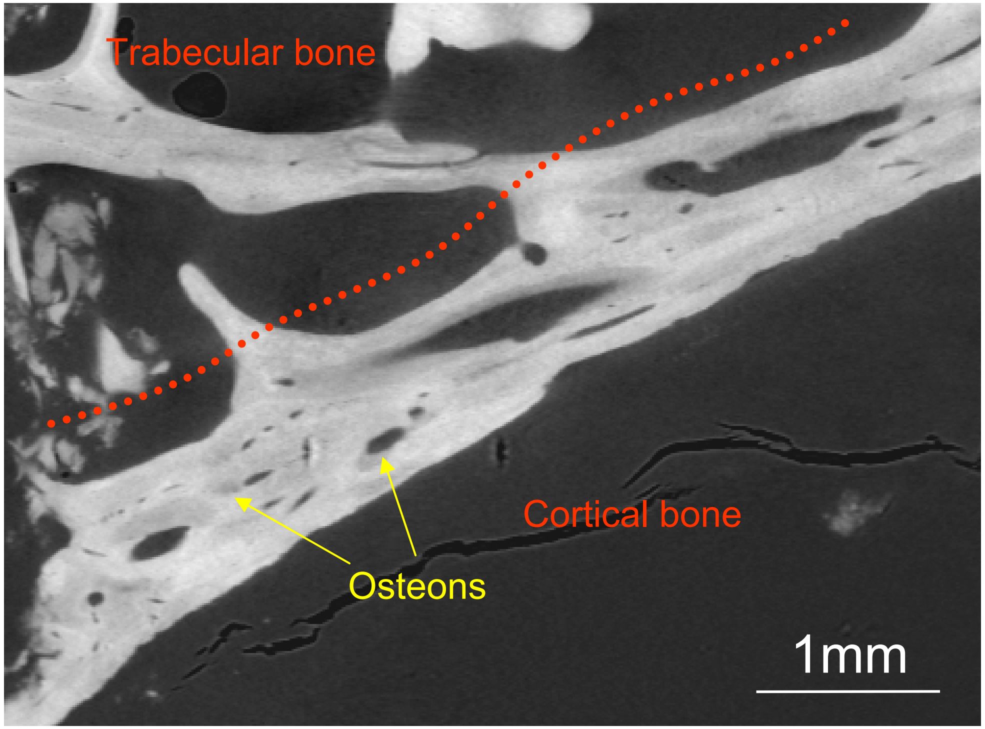

Monochromatic beam -> Reconstruction of linear attenuation coefficient μ

Quantification of 3D mineral content provided a suitable calibration

S. Nuzzo *et al.*, *Medical Physics* 29(11),2672-2681, 2002.
S. Nuzzo *et al.*, *Journal of Bone Mineral Research* 17(8), 1372-1382, 2002.

S. Nuzzo, ESRF ID19
F. Peyrin, CREATIS INSA Lyon & ESRF ID19

Quantitative µCT: Calibration procedure

Phantoms: homogeneous water solutions of various known K_2HPO_4 concentrations

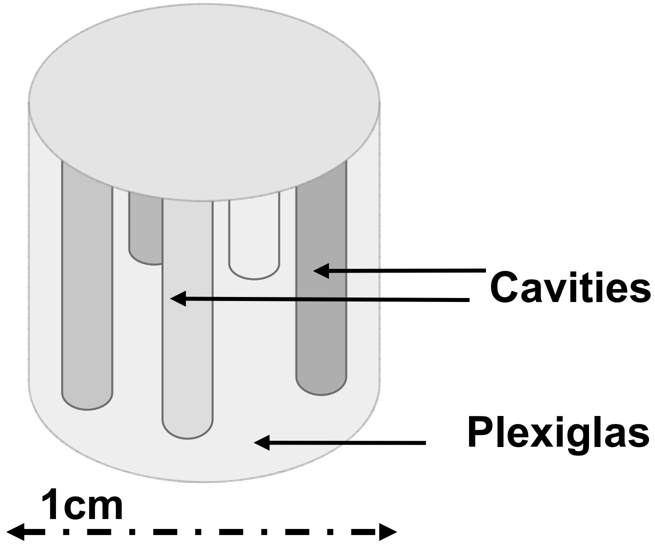

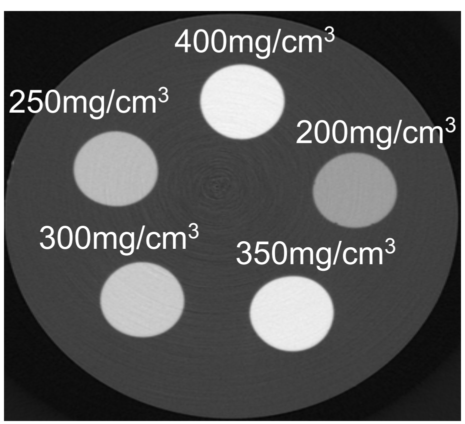

2D slice extracted from the 3D tomographic image of the phantom

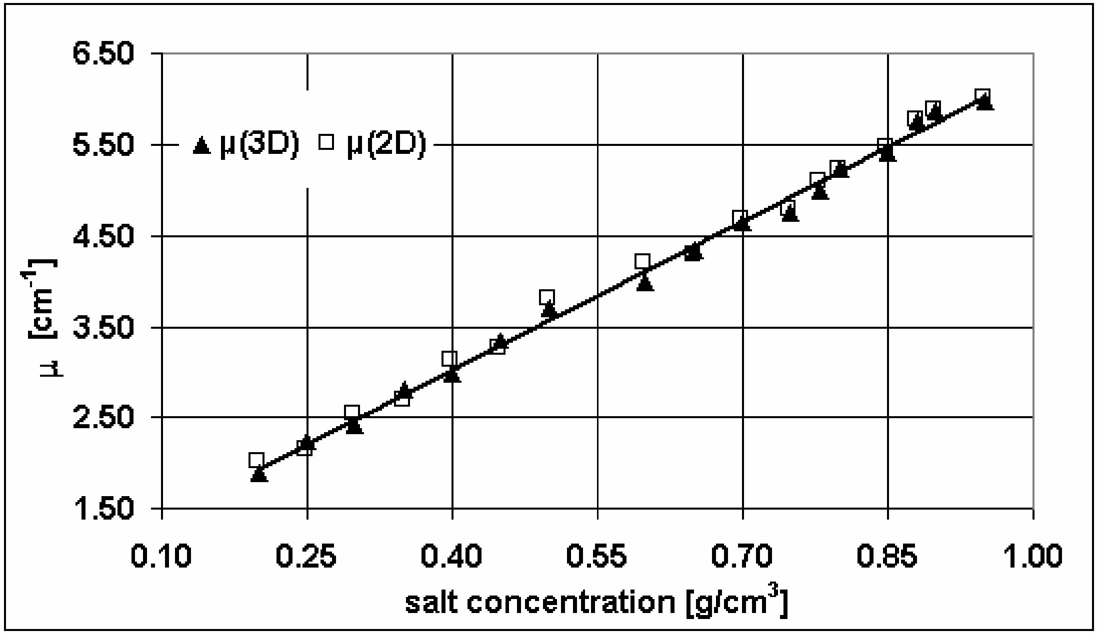

Calibration curve
Reconstructed linear attenuation coefficient <-> Bone mineral concentration

S. Nuzzo *et al.*, *Medical Physics* 29(11),2672-2681, 2002.

Comparison with micro-radiography : qualitative results

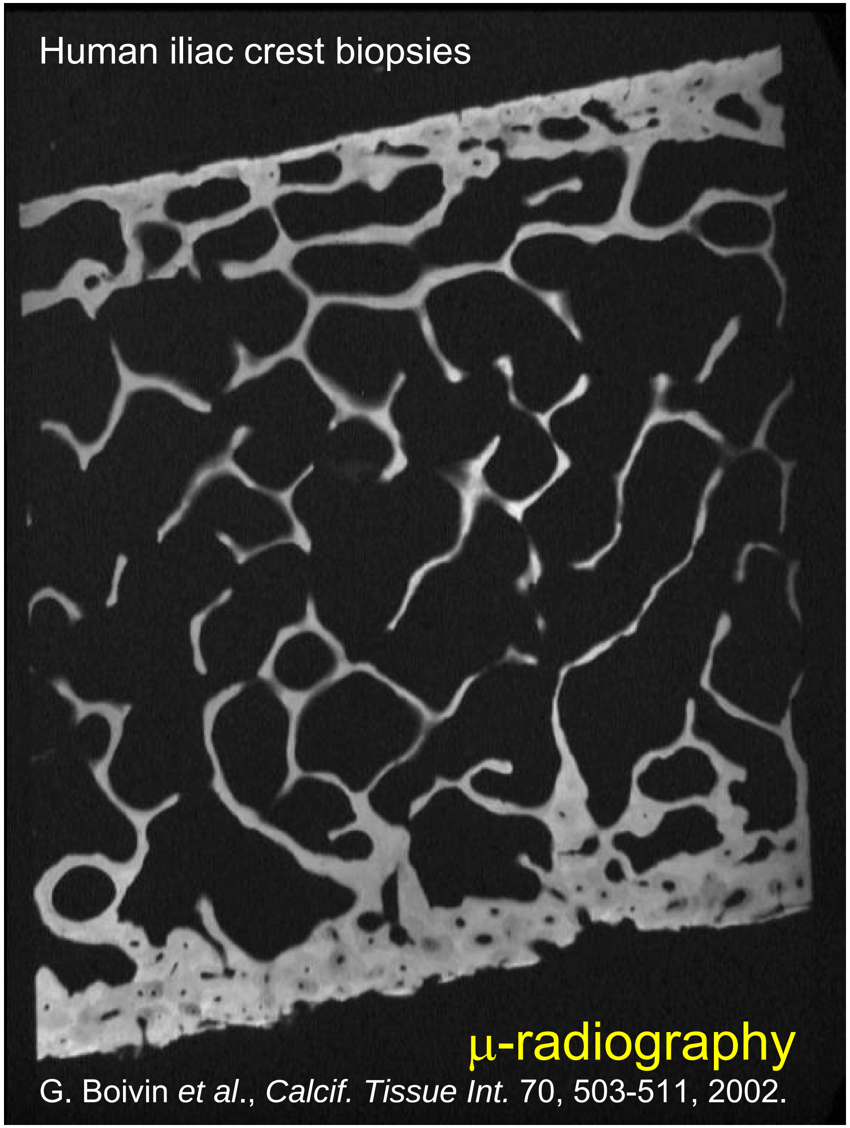

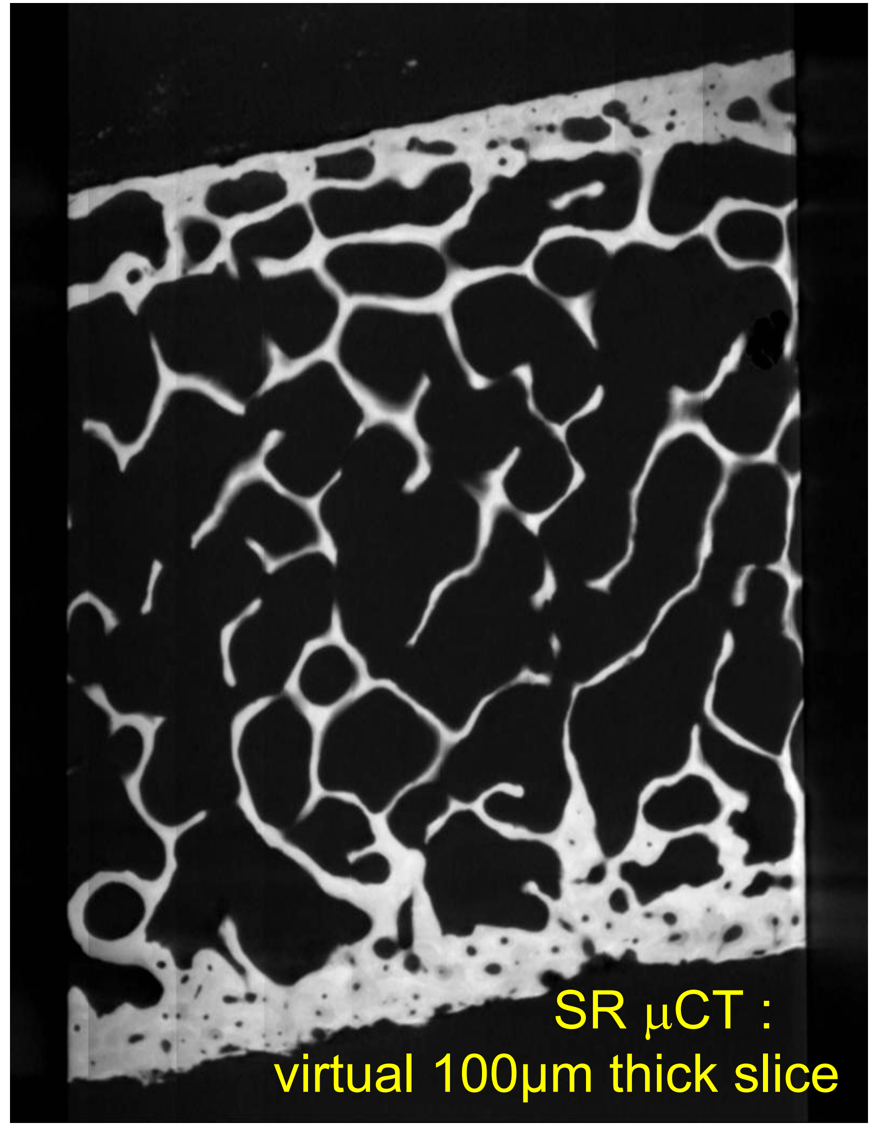

S. Nuzzo *et al.*, *Medical Physics* 29(11),2672-2681, 2002.

Comparison with micro-radiography : quantitative results

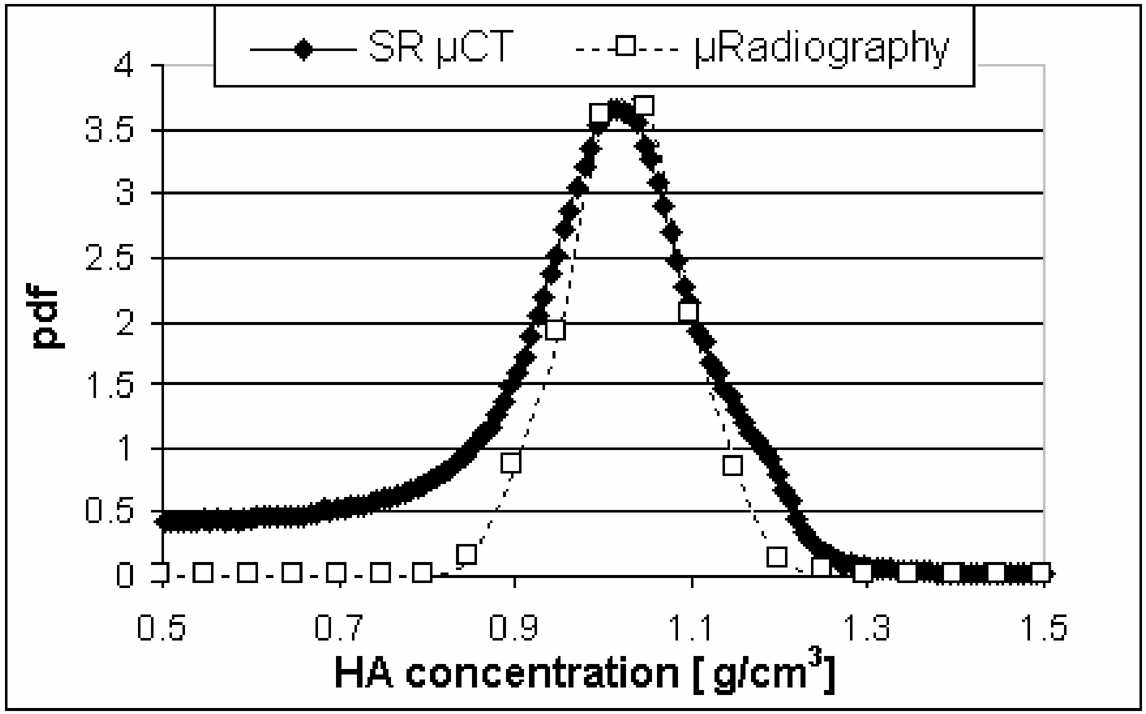

Degree of mineralization of bone (DMB) distribution measured by the two techniques

Repeated on 4 biopsies ⇨ Mean difference = 4.7 %

Slightly higher in trabecular than in cortical bone

S. Nuzzo *et al.*, *Medical Physics* 29(11),2672-2681, 2002.

S. Nuzzo, ESRF ID19

F. Peyrin, CREATIS INSA Lyon & ESRF ID19

Effects of a sequential Etidronate therapy in post-menopausal osteoporosis

- Iliac crest biopsies from 14 patients, before (baseline), after 1 year and after 2 years of treatment.
- Sequential 13 week therapy repeated 4 times :
  - Etidronate (Procter and Gamble) 400 mg/day for 2 weeks
  - Ca (Sandoz) 1g/day for 11 weeks
- Measurement of the 3D microarchitecture parameters and bone mineralization

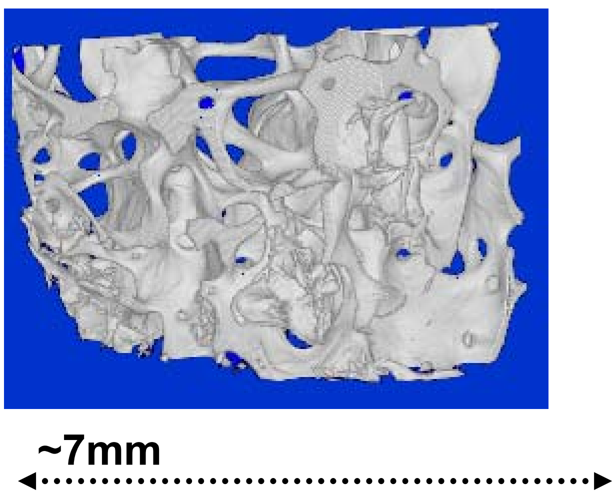

3D µCT image of an iliac crest biopsy

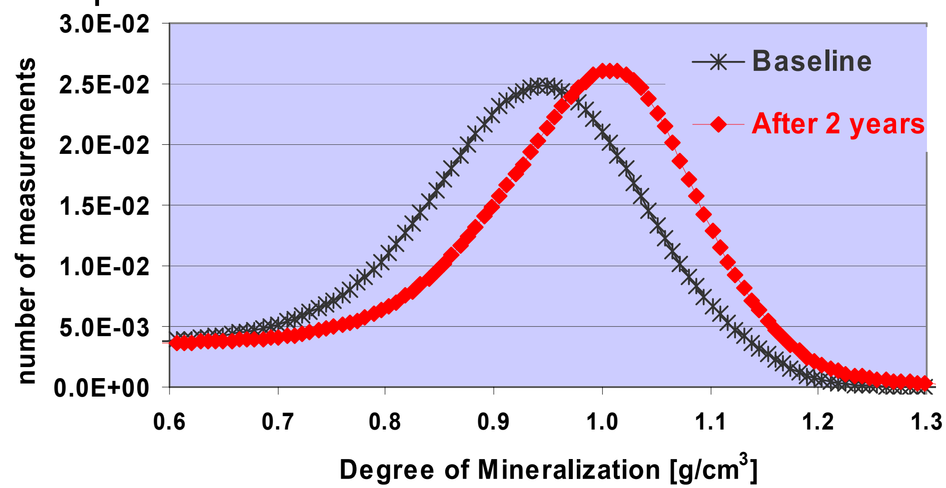

• Baseline → After 2 years :

↑ HA concentration 12% (cortical)

↑ HA concentration 8% (trabecular)

S. Nuzzo *et al.*, *Journal of Bone and Mineral Research* 17(8),1372-1382, 2002

S. Nuzzo, F. Peyrin, CREATIS INSA Lyon & ESRF ID19
M.H. Lafage-Proust, INSERM E9901, Saint-Etienne

In vivo imaging of bone micro-architecture in mice

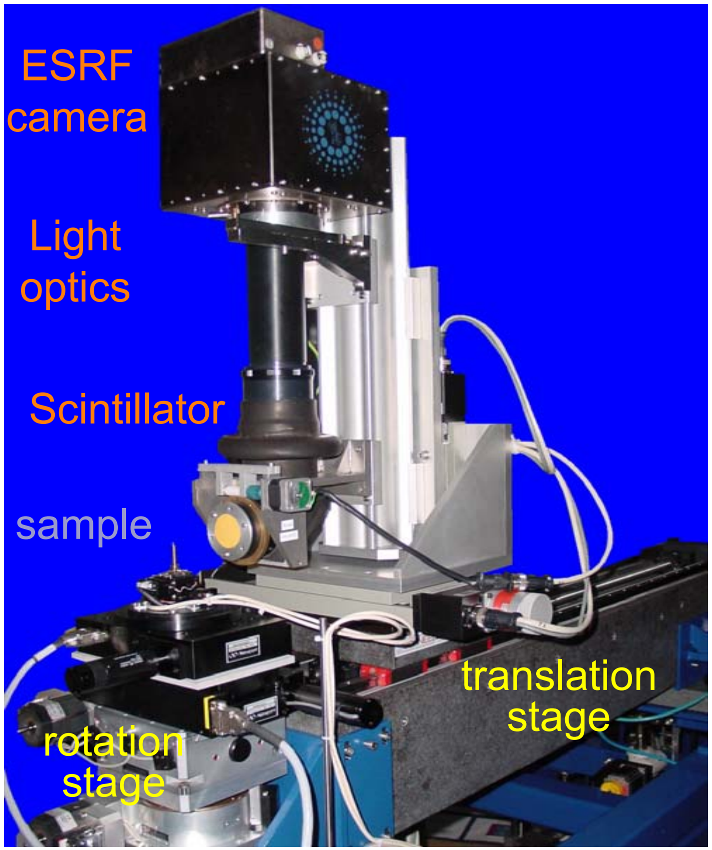

ID19 µCT setup

Animal holder

Projection

S. Bayat *et al.*, *Nuclear Instruments and Methods in Physics Research A* 548,247-252, 2005.

S. Bayat, ESRF
F. Peyrin, CREATIS INSA Lyon & ESRF ID19

In vivo imaging of bone micro-architecture in mice

voxel size : 10.13 µm

5 mn scan time

Transverse slice µCT image in the femur of a B6 mouse

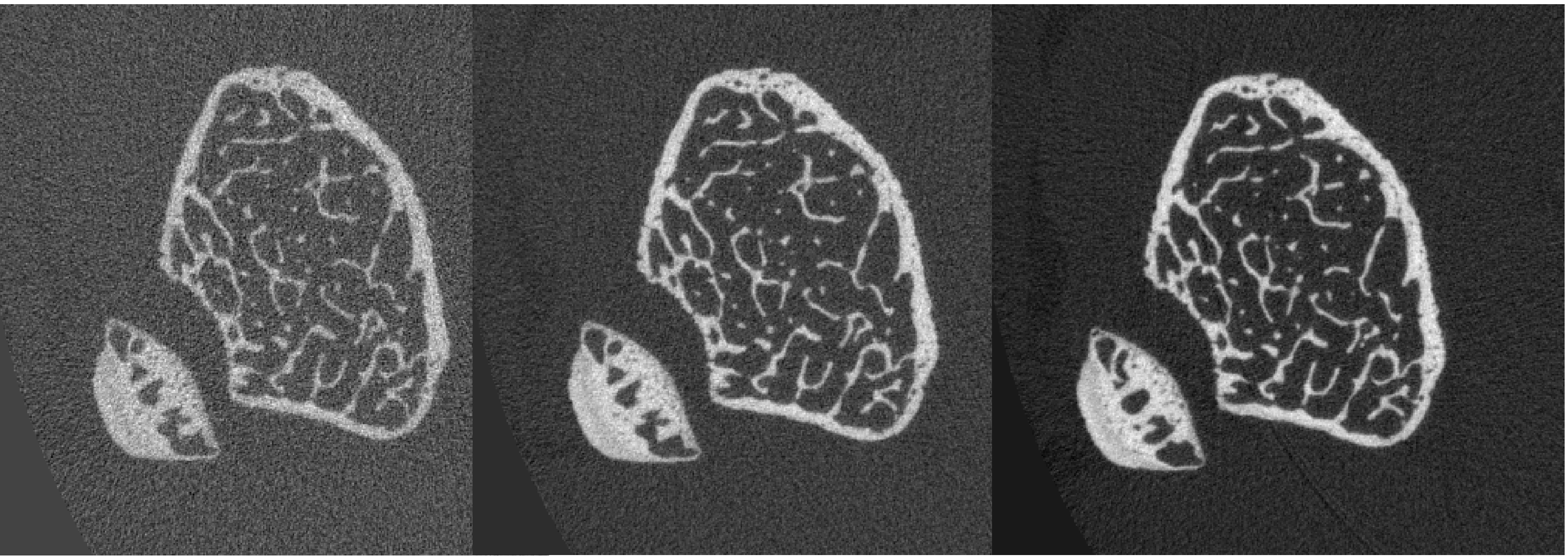

2.3 Gy	7.5 Gy	14.5 Gy
SNR : 8.3 (18.4dB)	11.2 (24.2dB)	24.3 (27.9dB)

S. Bayat *et al.*, *Nuclear Instruments and Methods in Physics Research A* 548,247-252, 2005.

4. Bone mineralisation

Bone mineral and possible substitutions

- Apatites

$$Me_{10}\,(XO_4)_6\,Y_2$$

Stoichiometric hydroxyapatite	Ca^{2+}	PO_4^{3-}	OH^-
Main possible substitutions	Sr^{2+}, Pb^{2+}, Cd^{2+}, Mn^{2+}, Na^+, La^{3+}, Mg^{2+}… vacancy: $\square$	HPO_4^{2-}, CO_3^{2-}, SO_4^{2-}, SiO_4^{3-} …	F^-, Cl^-, Br^-, CO_3^{2-}, O_2^{2-} … vacancy: $\square$

- Many forms of non-stoichiometric apatites
- Bone mineral: carbonated apatite $Ca_{8,3}\,\square_{1,7}\,(PO_4)_{4,3}\,(HPO_4, CO_3)_{1,7}\,(OH)_{0,3}\,\square_{1,7}$
- Adsorption and exchanges at the surface of the crystals
- Synthetic calcium phosphates are good models of bone mineral and offer similar physico-chemical properties.

Bone apatite maturation state using P and Ca K-edge µ-XANES

- Maturation of bone mineral and possible precursors of bone apatites are not well known yet.
- Better knowledge of bone mineralisation helpful for treatment of diseases like rickets, osteogenesis imperfecta or osteopetrosis.
- Local assessment of bone apatite maturation state using µ-XANES

XANES spectra of synthetic calcium phosphates at the Ca K-edge

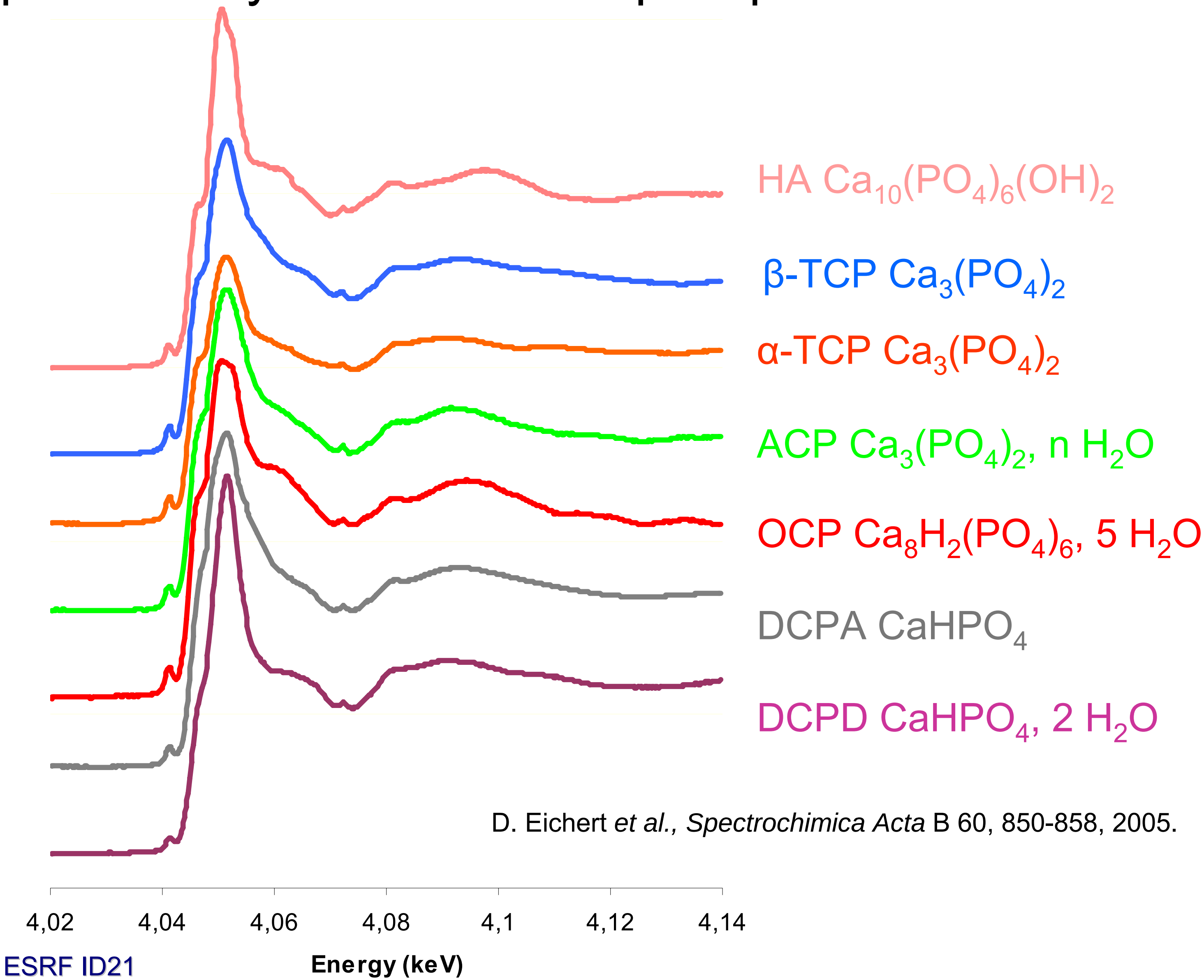

D. Eichert *et al., Spectrochimica Acta* B 60, 850-858, 2005.

D. Eichert, M. Salomé, ESRF ID21
C. Rey, CIRIMAT-ENSIACET, Toulouse

Follow-up of the maturation of poorly crystalline apatites using XANES at Ca K-edge

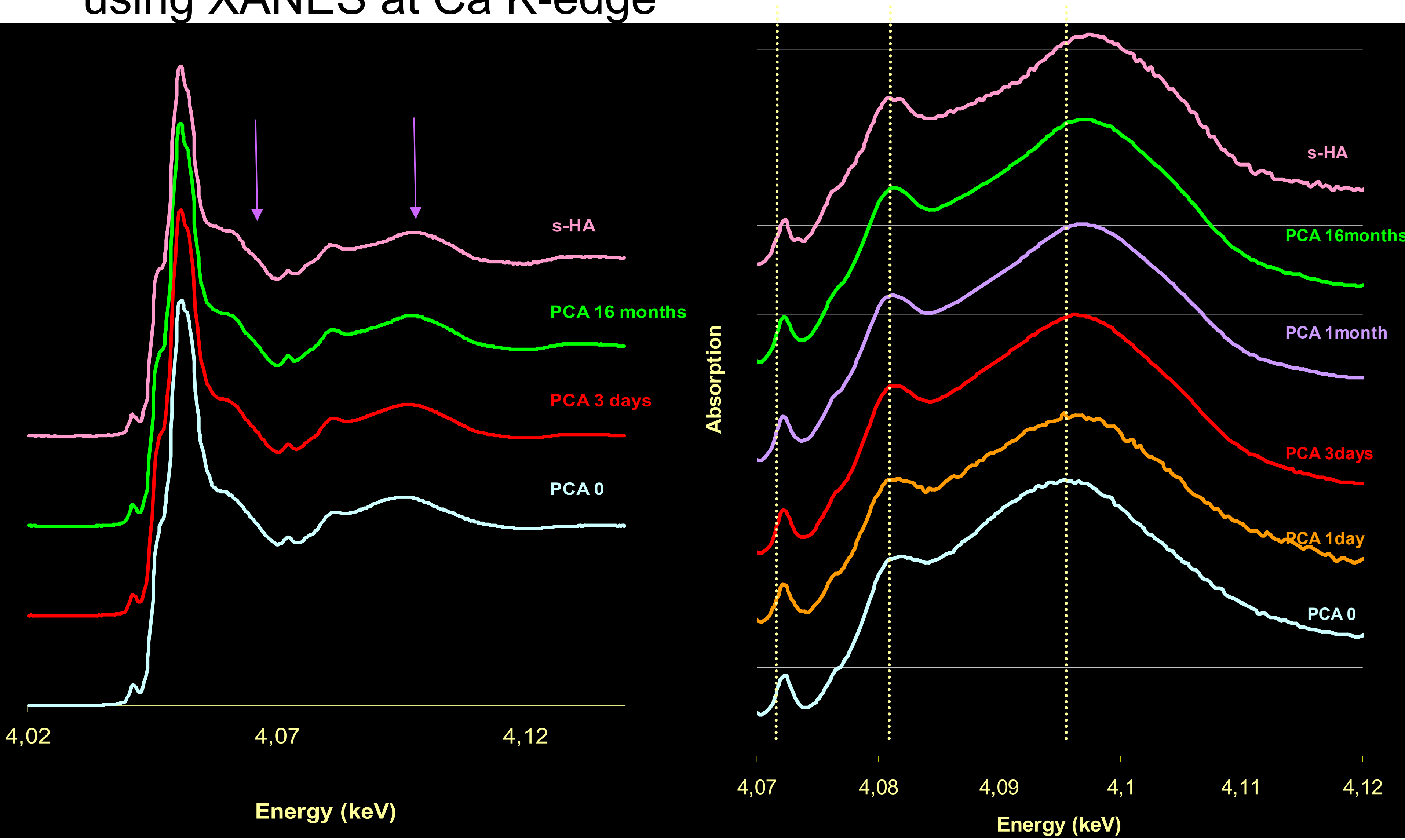

D. Eichert, M. Salomé, ESRF ID21
C. Rey, CIRIMAT-ENSIACET, Toulouse

D. Eichert *et al.*, *Spectrochimica Acta* B 60, 850-858, 2005.

Follow-up of the maturation of poorly crystalline apatites using XANES at Ca K-edge

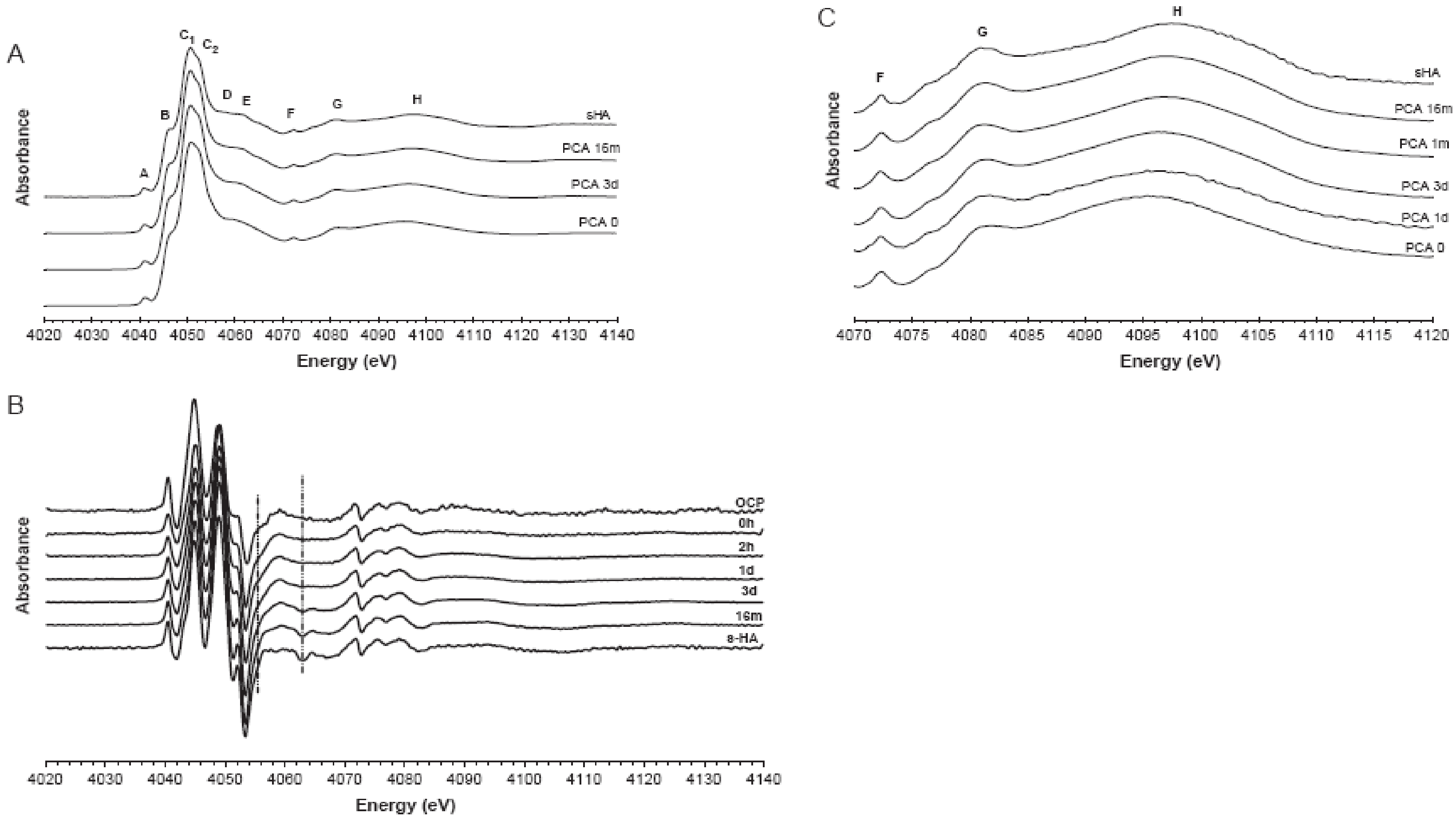

D. Eichert *et al., Spectrochimica Acta* B 60, 850-858, 2005.

D. Eichert, M. Salomé, ESRF ID21
C. Rey, CIRIMAT-ENSIACET, Toulouse

Follow-up of the maturation of poorly crystalline apatites using XANES at Ca K-edge

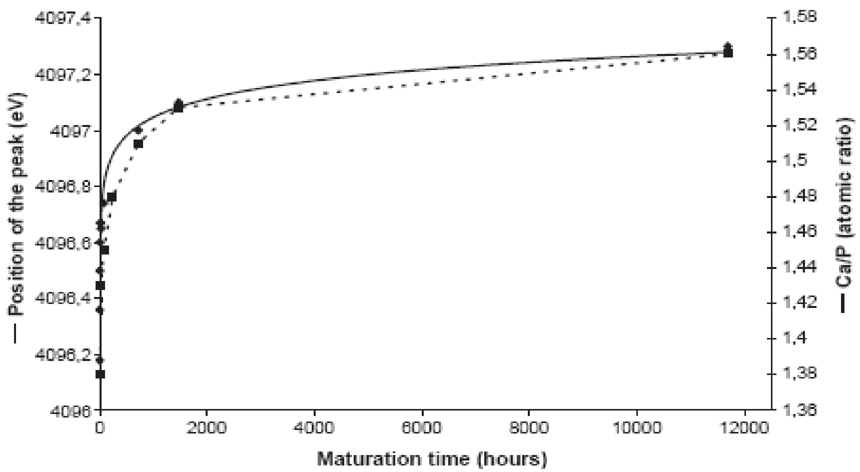

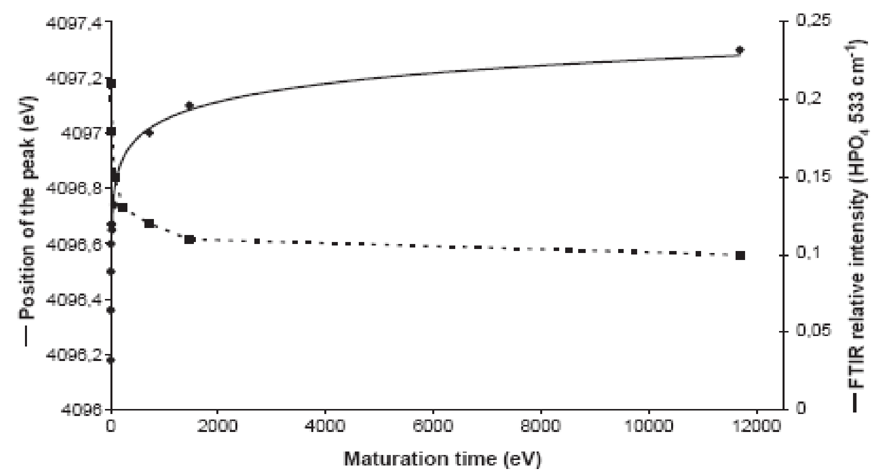

Correlation between maturation and modification of the XANES spectra
Technique sensitive to the modification of calcium and phosphorus environments

D. Eichert *et al., Spectrochimica Acta* B 60, 850-858, 2005.

D. Eichert, M. Salomé, ESRF ID21
C. Rey, CIRIMAT-ENSIACET, Toulouse

X-ray diffraction and bone

- X-ray diffraction
  - Crystal lattice in mineral crystallites
  - Identification of mineral phases

- Small Angle X-ray Scattering (SAXS) :
  - Orientation of the collagen fibers
  - Distribution of mineral crystallites
    - Shape
    - Thickness of the smallest crystallite dimension
    - Orientation, degree of alignment of the particles

- μ-SAXS mapping with micro-beams
  - 2D maps of bone crystallites properties

Please refer to:
P. Fratzl *et al.*, *Connective Tissue Research* 34(4), 247-254, 1996.
J.C. Hiller *et al.*, *Journal of Archaeological Science* 33, 560-572, 2006.

Micro-focus SAXS: 2D mapping of bone crystallites properties

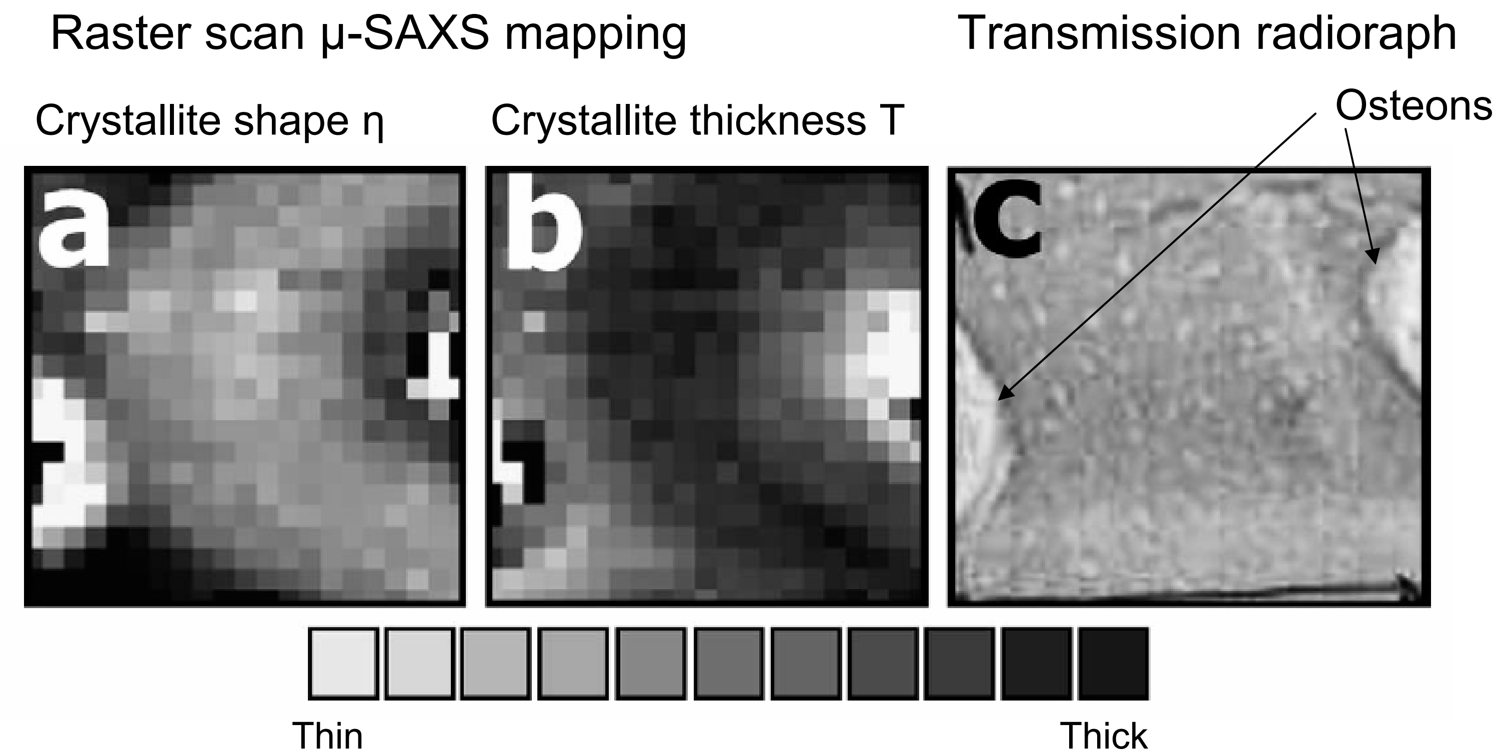

Modern human bone, 200 µm thick section

Applications in archaeological bone studies

J.C. Hiller *et al*., *Journal of Archaeological Science* 33, 560-572, 2006.

J. Hiller, Cardiff University

Experiment performed at ESRF ID18F

5. Biomechanics

In situ microtomography study of human bone under compressive stress

- Development of a micro-compression device compatible with µCT setup
- Analysis of microcracks origination, growth and propagation in 3D
- Study of bone biomechanical properties under dynamic strain

P. Bleuet *et al*, *Developments in X-Ray Tomography IV*. Edited by Bonse, Ulrich. Proceedings of the SPIE 5535, 129-136,2004.

In situ µCT study of human bone under compressive stress

ESRF

1. Excision

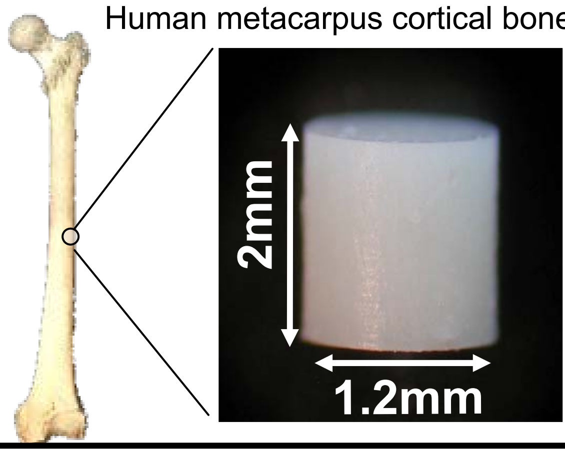

2. Data acquisition

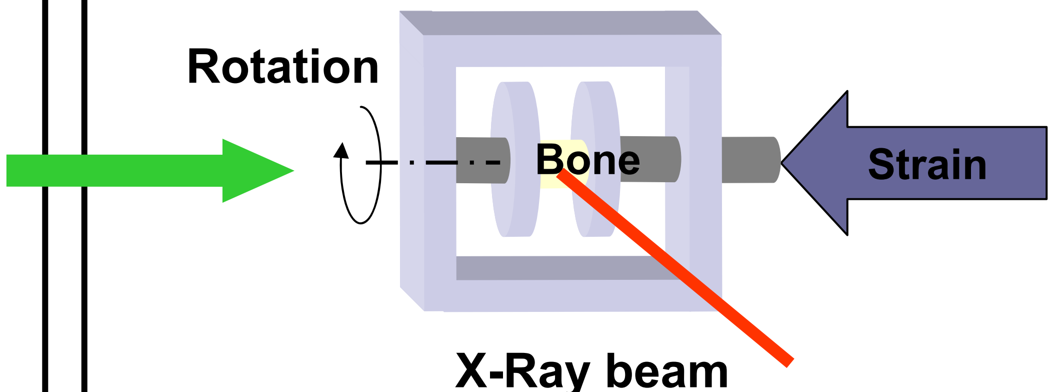

3. 3D Reconstruction and segmentation

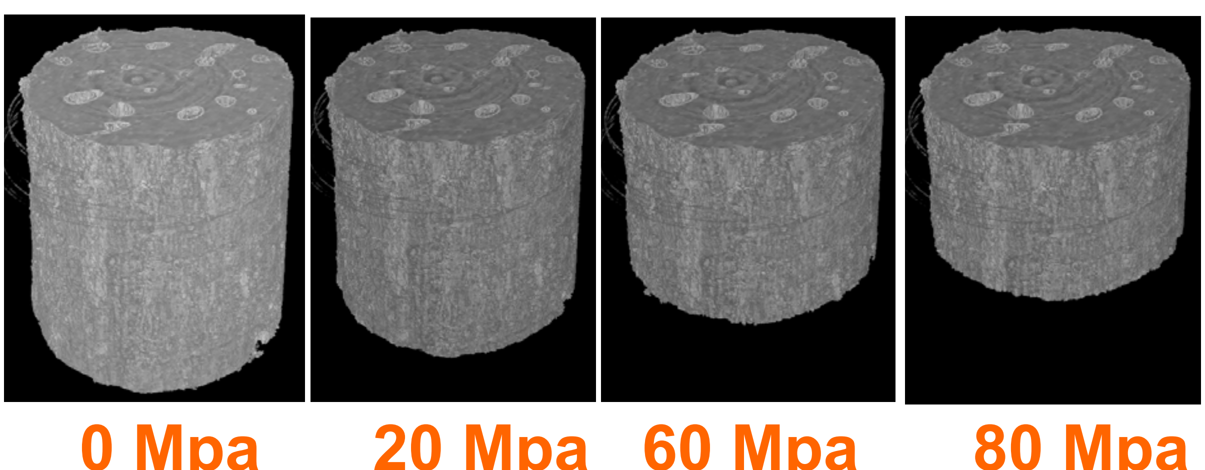

P. Bleuet *et al*, *Developments in X-Ray Tomography IV*. Edited by Bonse, Ulrich. Proceedings of the SPIE 5535, 129-136,2004.

P. Bleuet, ESRF ID22
J.P. Roux, G. Boivin, INSERM 403, Lyon

Micro-compression system for bone samples

Microscope for visible light sample observation during measurement

"Aérographe"

Motion gauge

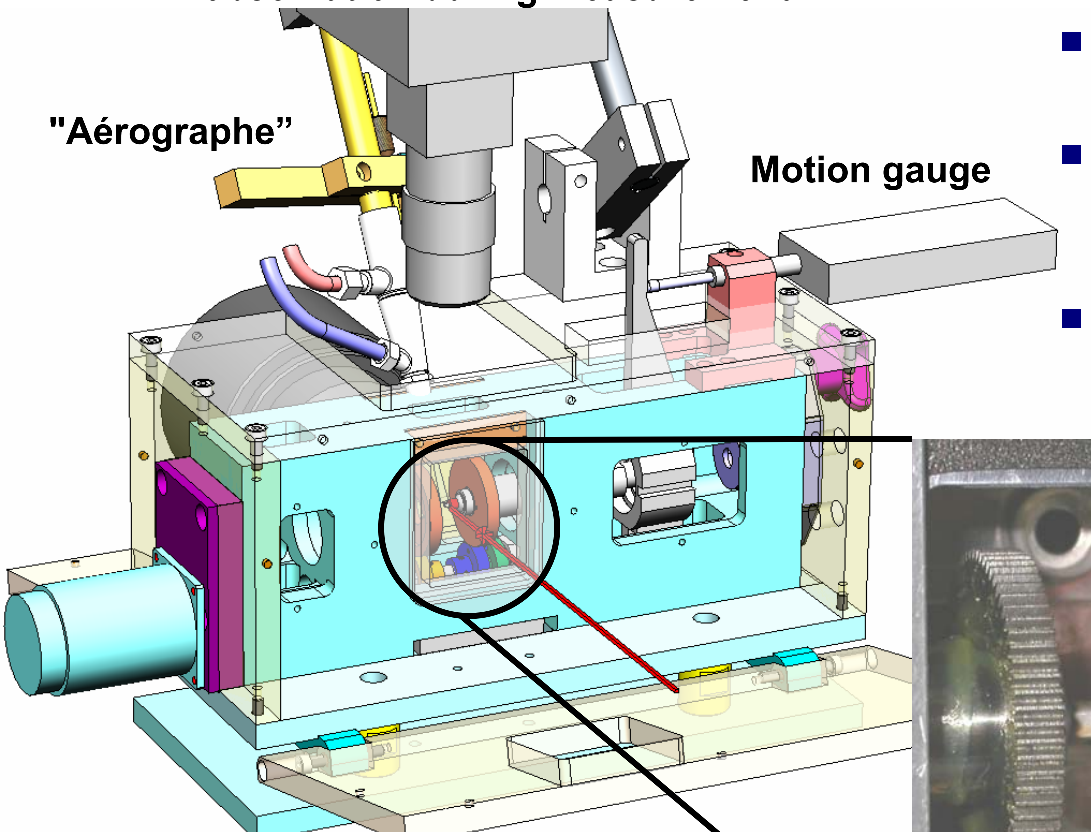

- Compatibility with µCT setup
- High accuracy rotation controlled by precision bearings
- Fatigue testing within 0 to 1% strain -> Sinusoidal motion with 5-10 µm amplitude using a piezoelectric actuator
- Measurement of (F,D): 2 motion gauges + 1 force gauge

Sample cell
Ex-vivo physiological conditions
T=37°C H=100%

Design by Y.Dabin, ESRF Technical Services

P. Bleuet, ESRF ID22
J.P. Roux, G. Boivin, INSERM 403, Lyon

In situ microtomography study of human bone under compressive stress

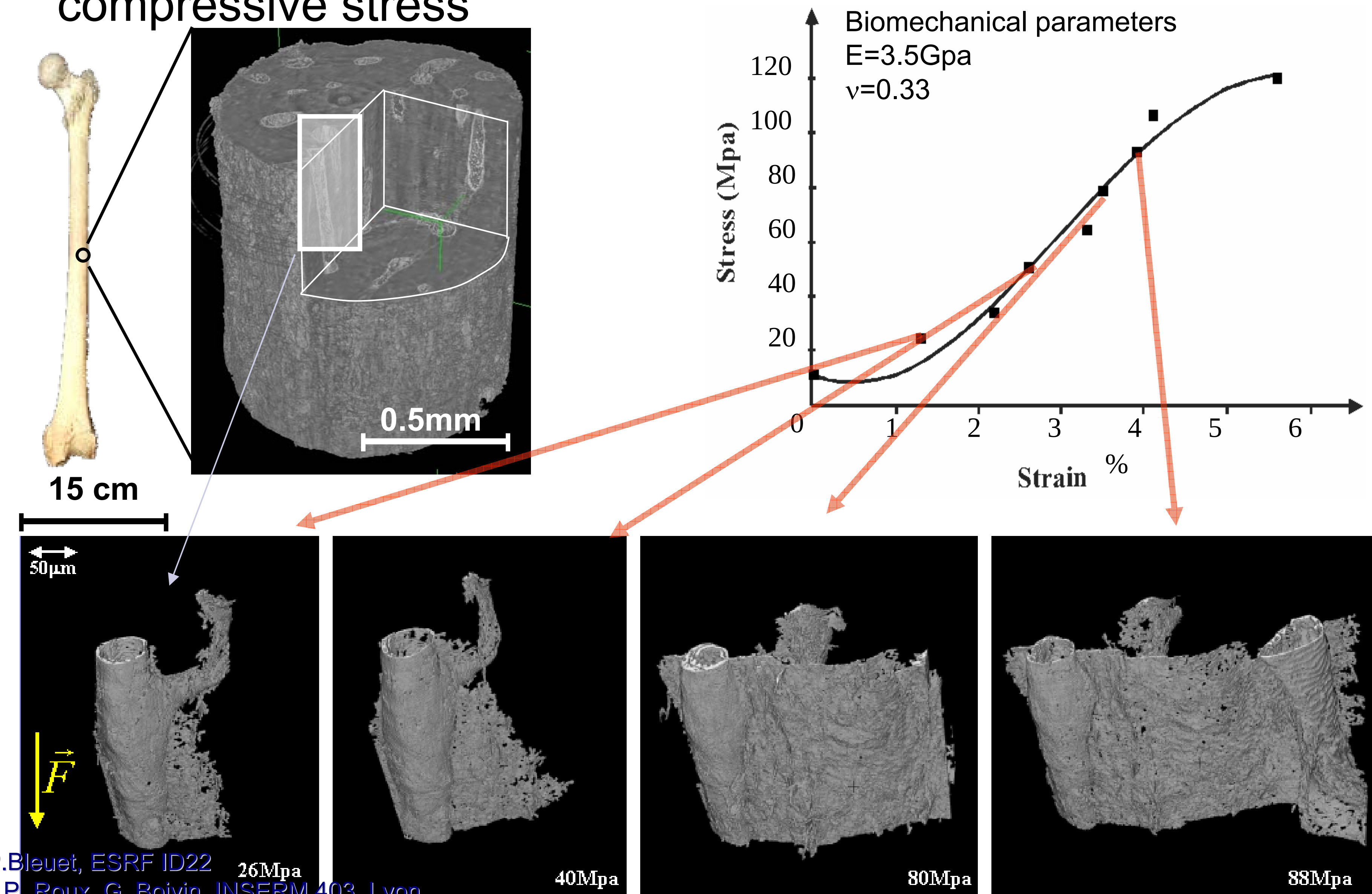

P.Bleuet, ESRF ID22
J.P. Roux, G. Boivin, INSERM 403, Lyon

6. Metals accumulation in bone

Metals accumulation in bone

- Easy storage and exchange of metals in bone
- May induce mineralisation defects
- Effects often dose-dependent
- Metals issued from
  - Food
  - Therapy (La, Sr, …)
  - Environment contamination (Pb, Cr, …)
  - Release from metallic implants (Ti, Co, Fe, Cr, …)
- Assessment of trace metals accumulation sites and potential toxicity
- µ-fluorescence (µXRF) mapping
  - High sensitivity (a few ppm)
  - Chemical speciation in µ-XANES

μ-XRF mapping of La in bone of chronic renal failure rats

- Accumulation of phosphate in Chronic Renal Failure patients (CRF)
- To decrease serum phosphate level: use of phosphate binders
  - Aluminum hydroxide Al(OH3)
  - Calcium carbonate $CaCO3$
  - Side effects: Al mineralization defects, Ca extra-osseous calcification
- Alternative: Lanthanum carbonate
- Check possible effect on bone mineralization, possible accumulation in bone tissue, tissue localization is important

µ-XRF mapping of La in bone of chronic renal failure rats

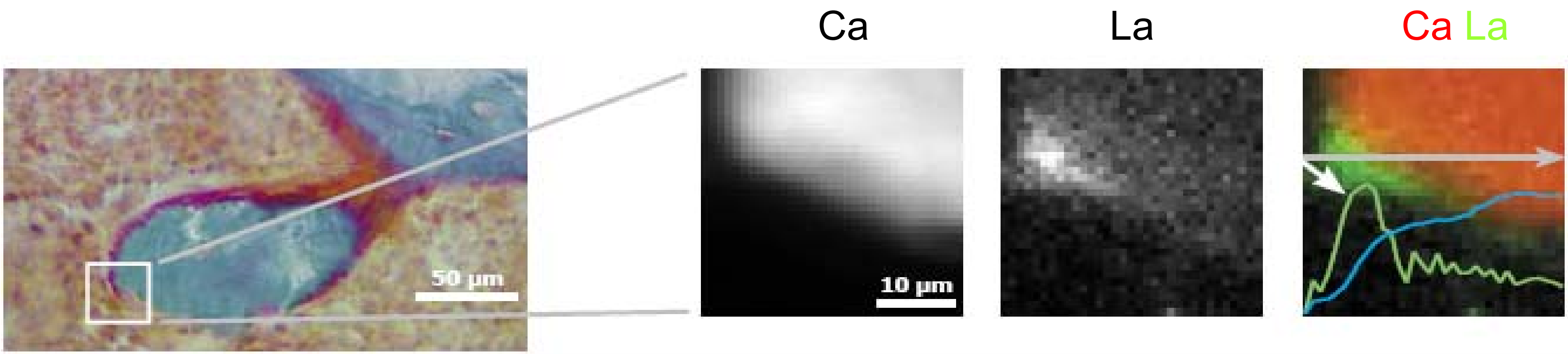

Goldner stained adjacent slice (500x)
Osteoid tissue: red, Mineralised bone: blue

10µm thick trabecular bone section.
E=6.3 keV, 36 µm x 32 µm, 1 µm step size, 5s/pixel

Chronic renal failure rat model (5/6 nephrectomy) loaded with daily oral doses of lanthanum carbonate (2g/kg/day) over a 12 week period.

G. Behets *et al.*, *Kidney International* 67, 1830-1836, 2005.

G. Behets, S.C. Verbeckmoes, P. D'Haese, M. E. De Broe, Department of Nephrology, Antwerp University
M. Salomé, ESRF ID21

Localisation of La in different types of renal osteodistrophy

Animal with normal bone histology
Bulk La concentration 2.68 µg/g

Animal showing hyperparathyroid bone disease
Bulk La concentration 2.71 µg/g

Animal with a mineralization defect
Bulk La concentration 2.81 µg/g

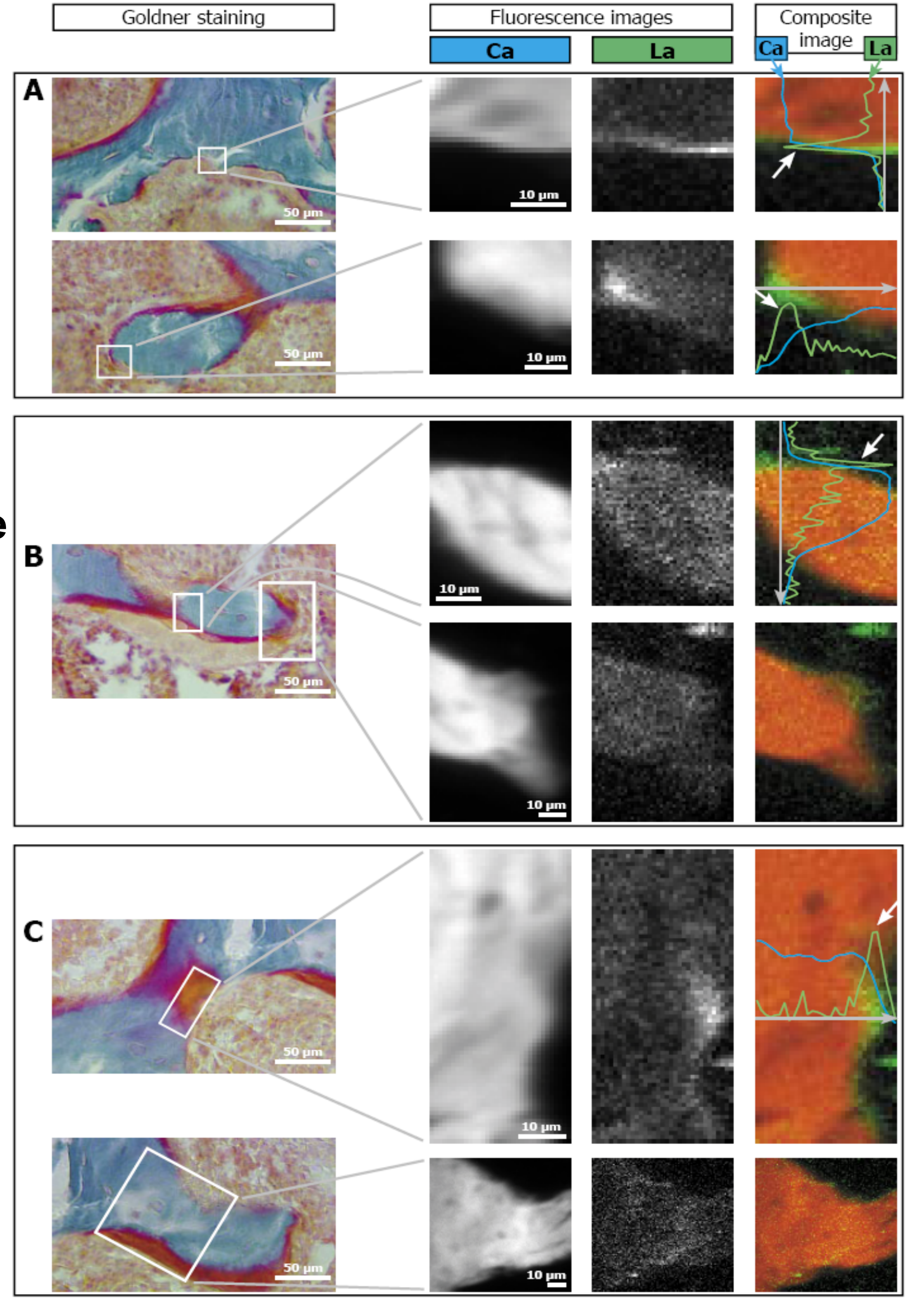

Conclusions:

- La generally at the outer edge of mineralized bone both at active and quiescent sites
- No obvious relationship between osteoid amount or type of renal osteodistrophy
- After a 2-4 weeks washout period: same localization of La, no more mineralization defect

G. Behets *et al.*, *Kidney International* 67, 1830-1836, 2005.

7. Orthopedics and Biomaterials

Diffraction Enhanced Imaging (DEI) of bone

Diffraction Enhanced Imaging of joint cartilage

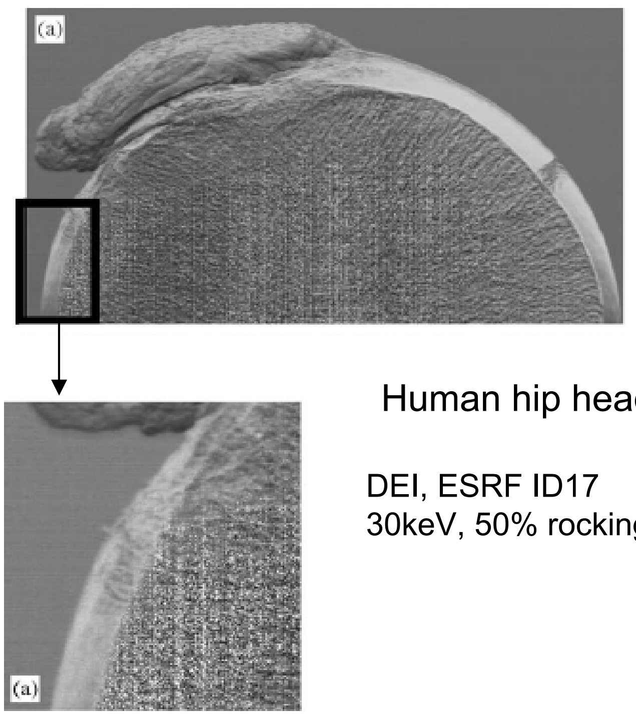

Human hip head

DEI, ESRF ID17
30keV, 50% rocking curve

A. Wagner *et al*., *Nuclear Instruments and Methods in Physics research A* 548, 47-53, 2005.

Identification of the quality of bone ingrowth into HA layer of implant

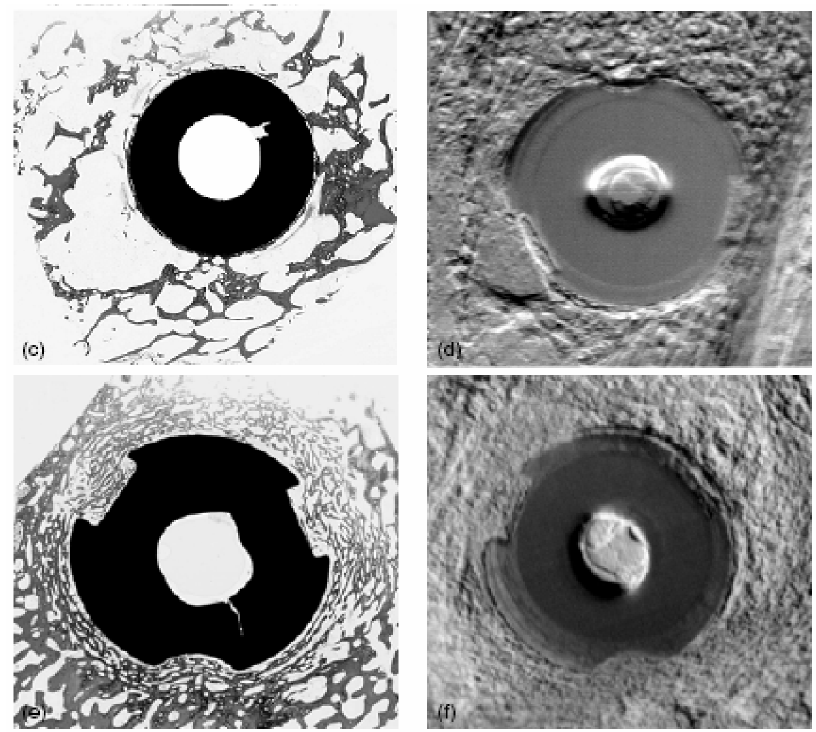

Histological section

DEI, ESRF ID17
50keV, 15% rocking curve

Titanium implant integration in sheep, 9 week post-surgery

A. Wagner *et al*., *Physics in Medicine and Biology* 51(5), 1313-1324, 2006.

Kinetics of bone deposition into porous calcium phosphate scaffolds

Highly porous hydroxyapatite scaffolds seeded with bone marrow stromal cells, implanted in immunodeficient mice.

8 weeks | 16 weeks | 24 weeks implantation

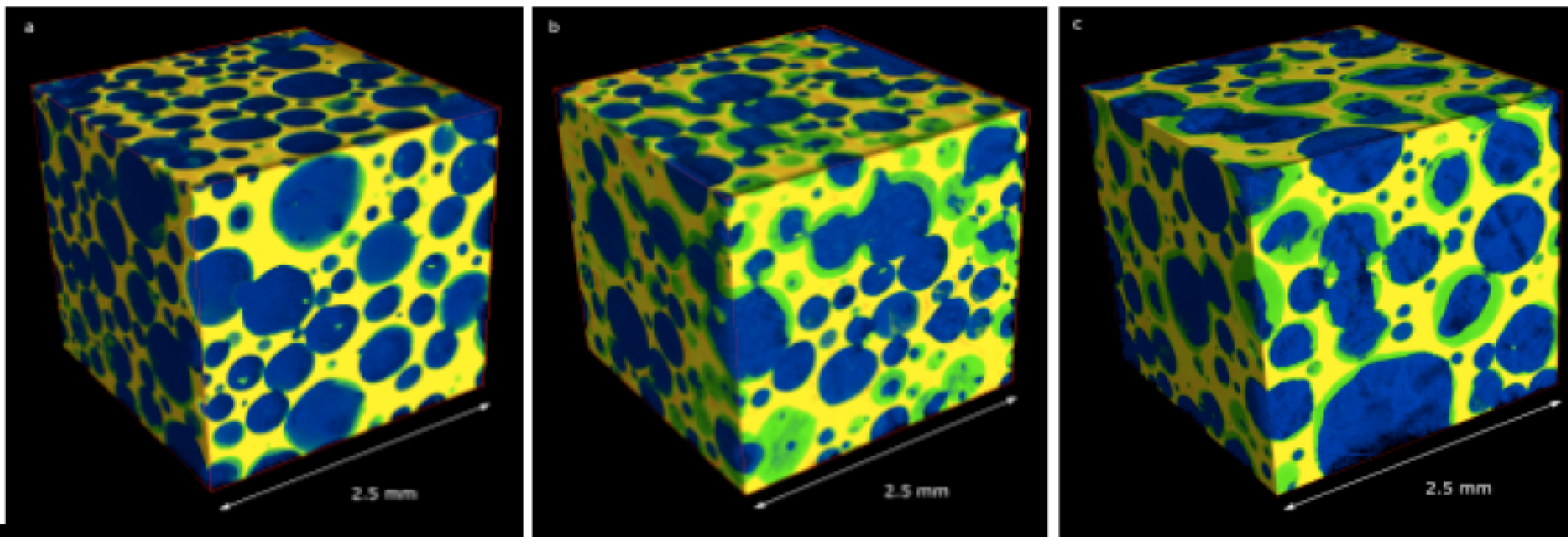

Newly formed bone
Inner surface of scaffold
Soft tissues

V.S. Komlev *et al.*, *Tissue Engineering* 12(12),3449-3458, 2006.

V.S. Komlev, Universita Politecnica delle Marche and CNISM, Ancona, Italy & Institute for Physical Chemistry of Ceramics, Russian Academy of Sciences, Moscow, Russia
F. Peyrin, CREATIS INSA Lyon & ESRF ID19

Kinetics of bone deposition into porous calcium phosphate scaffolds

Histogram of absorption coefficient in the 3D µCT image

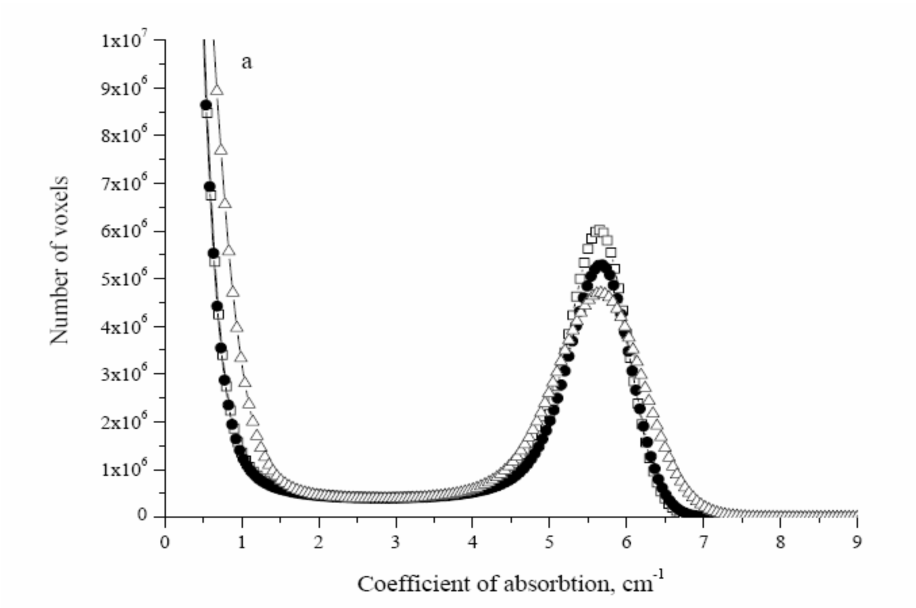

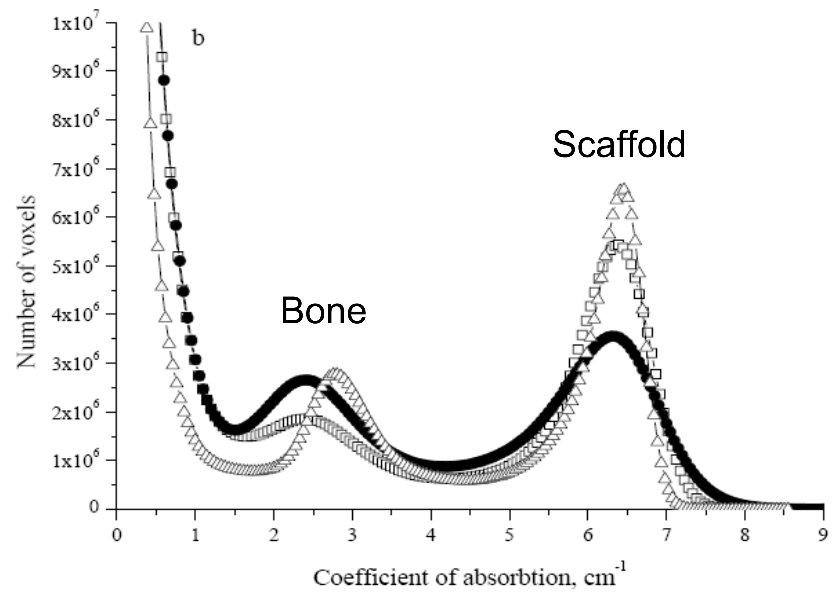

Scaffold before implantation

Scaffold + newly formed bone after:
□ 8 weeks,
● 16 weeks,
Δ 24 weeks implantation

V.S. Komlev *et al*., *Tissue Engineering* 12(12),3449-3458, 2006.

V.S. Komlev, Universita Politecnica delle Marche and CNISM, Ancona, Italy & Institute for Physical Chemistry of Ceramics, Russian Academy of Sciences, Moscow, Russia
F. Peyrin, CREATIS INSA Lyon & ESRF ID19

Osseo-integration of silicon-stabilized tricalcium phosphate bioceramics

- Silicon-stabilized tricalcium phosphate bioceramics (Millenium Biologix Corp., Canada) 67% Si-TCP, 33% HA/β-TCP, seeded with bone marrow stromal cells.
- Implanted in immuno-deficient mice for 8 or 24 weeks

Decrease of scaffold thickness, increase of bone thickness

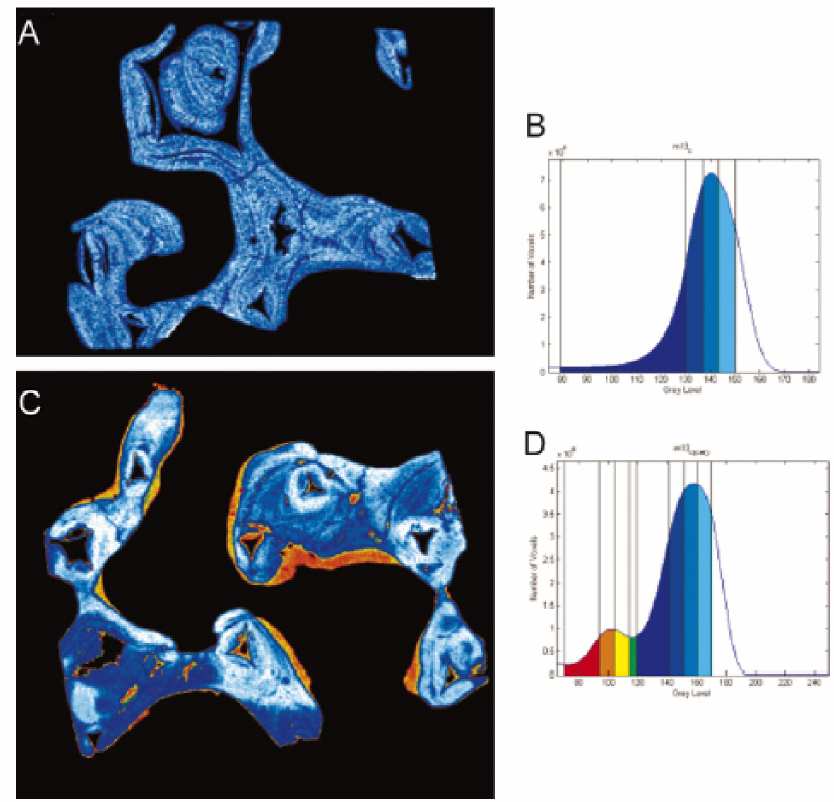

μ-CT images (ESRF ID19) of scaffold before and after 24 weeks implantation

M. Mastrogiacomo *et al*., *Biomaterials* 28(7), 1376-1384, 2007.

Osseo-integration of silicon-stabilized tricalcium phosphate bioceramics

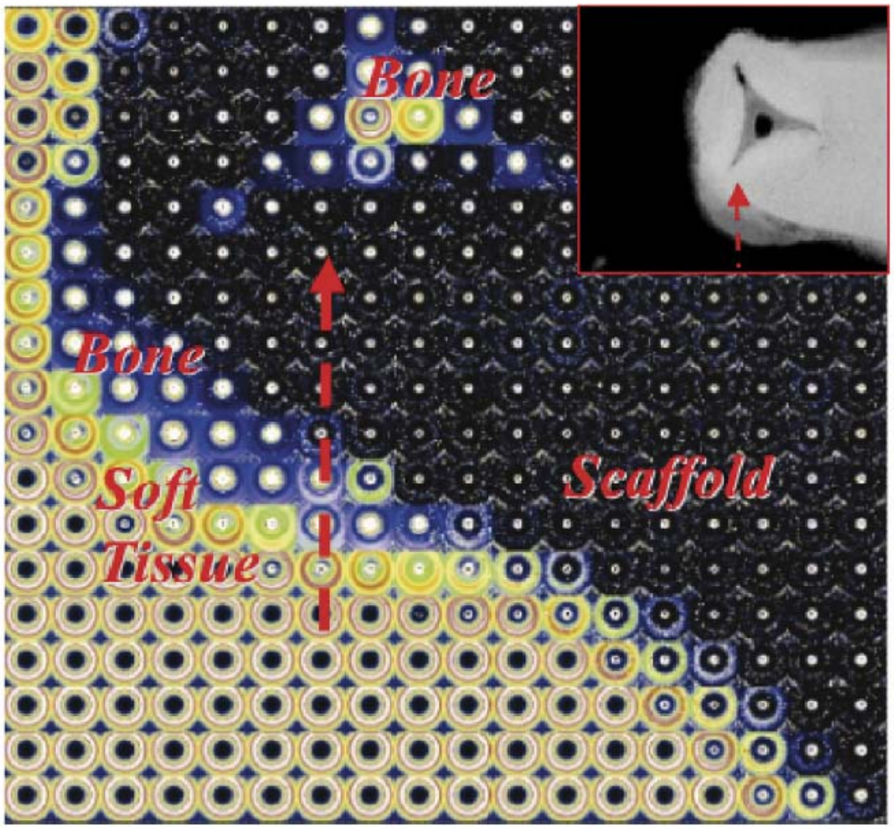

μ-diffraction images (ESRF ID13) of scaffold after 8 weeks implantation in immuno-deficient mouse

- Mapping of the variation of the scattered intensity of different phases:
  - HA in newly formed bone
  - HA in scaffold
  - TCP in scaffold

M. Mastrogiacomo *et al.*, *Biomaterials* 28(7), 1376-1384, 2007.

8. FTIR micro-spectroscopy

A brief reminder about FTIR spectroscopy

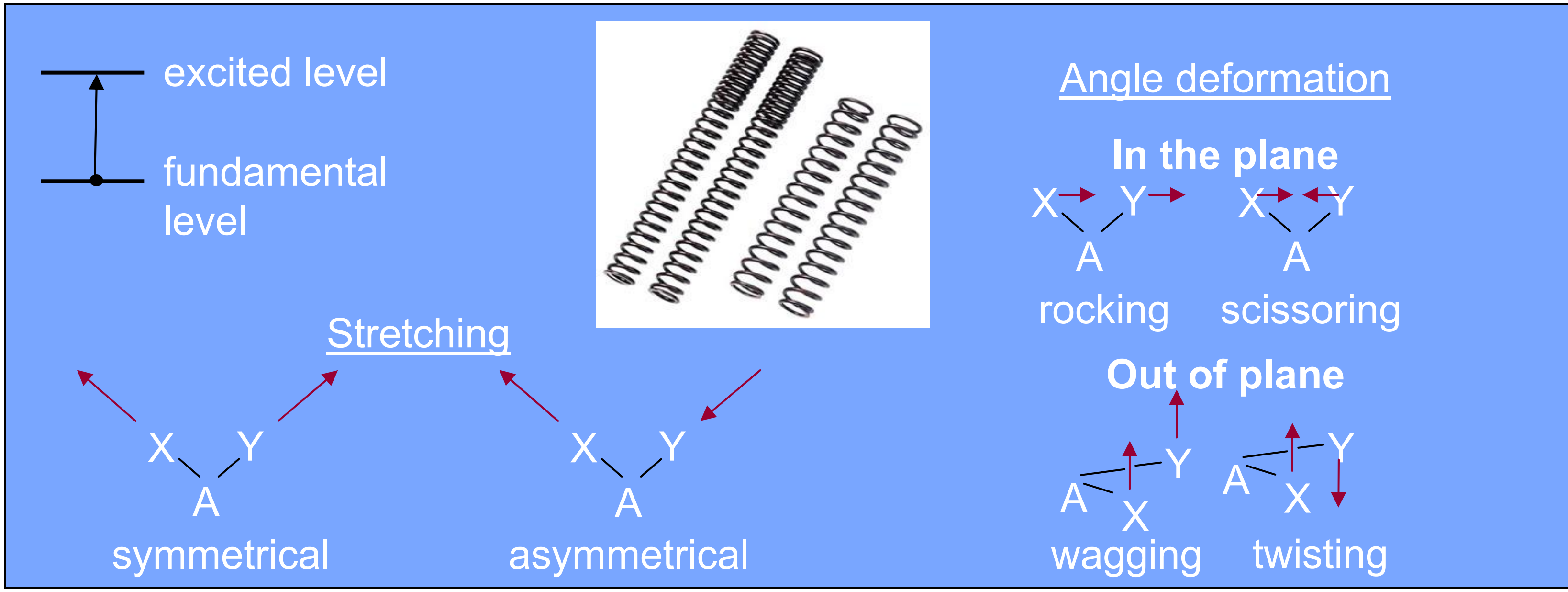

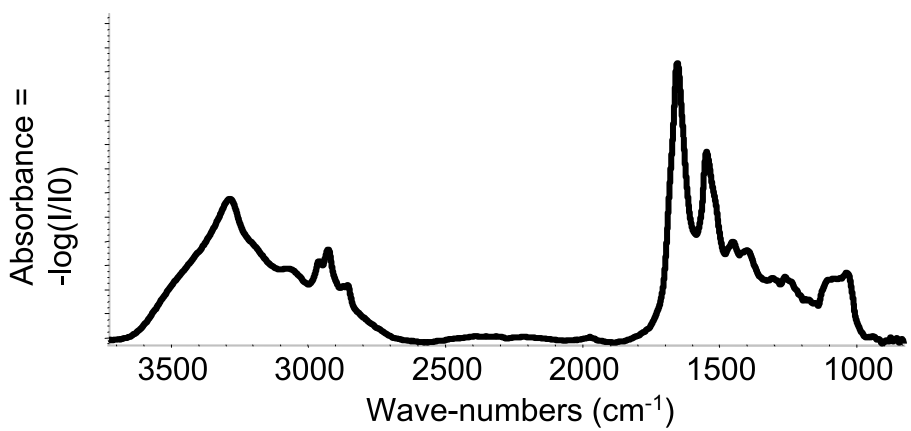

Molecular and structural information

Fourier-Transform Infra-Red Spectroscopy of bone

- Physico-chemical characterization of bone apatite
- Nature of the mineral phases
- Determination of relative amount of mineral / matrix
- Mineral crystallinity and maturity
- Nature of substituents and sites in apatite structure
- Environment of the ions
- Matrix composition

Bone FTIR spectrum

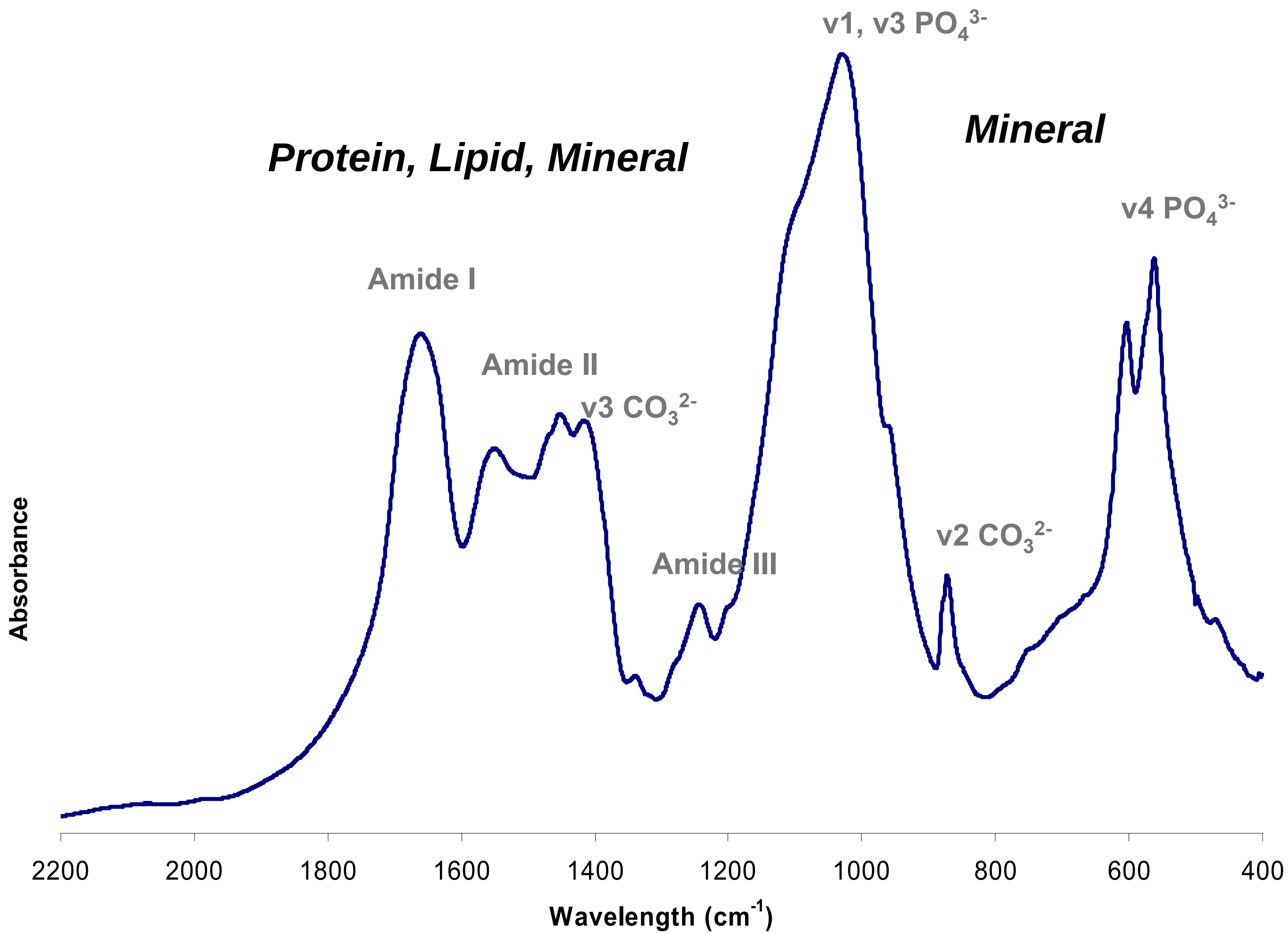

FTIR spectrum of trochanter bone

D. Eichert, ESRF ID21

Main FTIR absorbance bands in bone

Bands	Wavenumbers	Information
v1,v3 PO_4^{3-} bands	900 – 1200 cm-1	Crystal maturity
Amide I bands	1590 - 1720 cm-1	Organic phase
v4 PO_4^{3-} bands	500 – 650 cm-1	Crystallinity
v2 CO_3^{2-} bands	878 cm-1	Type A carbonate *Substitution OH^- site*
	871 cm-1	Type B carbonate *Substitution PO_4^{3-} site*
	866 cm-1	Labile surface carbonate

Please refer to:
C. Rey et al., *Cells Mater*. 5, 345-356, 1995.
H.M. Kim *et al*., *Calcified Tissue International* 59, 58-63, 1996.
A.L. Boskey *et al*., *Calcified Tissue International* 72, 533-536, 2003.
L. Miller *et al., Biochimica et Biophysica Acta 1527*, 11-19, 2001.

FTIR Micro-spectroscopy mapping of biomaterial integration

Visible light image

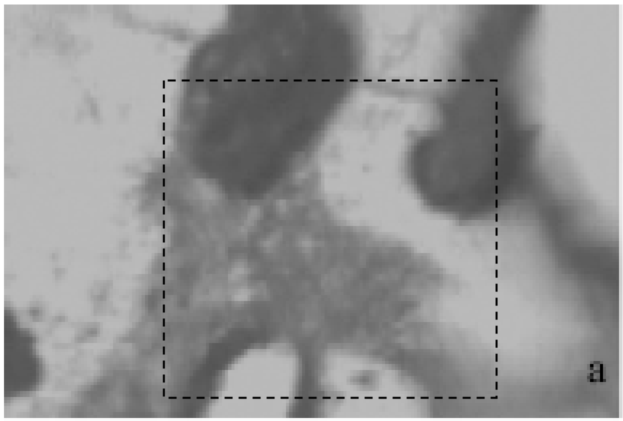

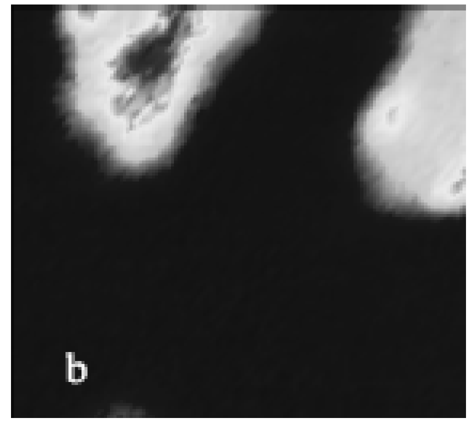

Biomaterial
v_L OH band of HA
630 cm^{-1}

Bone
v2 CO_3^{2-} bands
878 cm^{-1}, 871 cm^{-1}

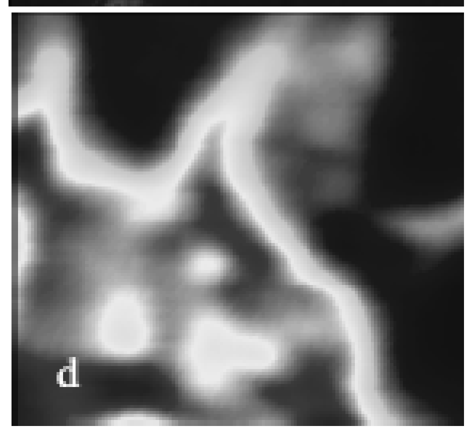

Organic matrix

HA cement implanted in rat tibia for 3 weeks

ID21 FTIR microscope
Aperture: 10x10 µm; Step size: 3 µm, 128 scans

D. Eichert *et al*., *Proceedings 8th International Conference on X–ray Microscopy, IPAP Conf series 7*, 210-212, 2006.

9. Perspectives

Future – Pushing further the spatial resolution …

- Development of imaging techniques at nano-scale
  - Nano-tomography
- Development of nano-probes
  - Nano-fluorescence
  - Nano-spectroscopy
  - Nano-diffraction
- Development of dedicated sample environments for *in situ* experiments
  - Under stress/strain
- Multi-modal approach combining techniques